

Novel methodology to determine the optimal energy storage location in a microgrid and address power quality and stability

L. F. Montoya
Student Member,
IEEE

Q. Fu
Student Member,
IEEE

A. Nasiri
Senior Member,
IEEE

V. Bhavaraju,
Senior Member,
IEEE

D. Yu
Senior Member,
IEEE

Abstract

In this paper, new voltage sensitivity indexes are proposed to search and evaluate the candidate buses in a microgrid, where the energy storage systems can be installed to contribute most effectively to the system. These indexes are derived from the inverse Jacobian matrix from the Newton-Raphson power flow analysis. After calculating and evaluating these indexes for the studied microgrid, four candidates' buses are selected. To verify that the selected buses are the best, the selected cases are simulated in PSCAD. The results from the proposed methodology and case studies have a consistent conclusion that the proposed voltage sensitivity indexes imply potential candidates for energy storage locations. Finally, by running a 24-hour time-sequence simulation of the complete system modeled in PSCAD, the best location is confirmed.

Introduction

Microgrids are receiving much attention recently because of their ability to provide higher energy surety, quality, and security while also providing sustainability and energy efficiency. A microgrid is defined as a network of loads and local generations (distributed generations), as well as energy storage systems. Mainly, the presence of energy storage systems enables microgrids to regulate their voltage and frequency while the system operates in various modes, such as when a microgrid is islanded from the utility grid. Further, due to the increasing penetration of renewable energy, which brings power intermittency into the microgrid, maintaining the system at a stable mode of operation is an issue.

Various researchers are focusing on power management and control strategies of energy storage systems within microgrids to improve a system's stability. However, in addition to the controls, the physical placement of energy storage elements in the system must be studied. A few papers discuss this issue from different perspectives. Paper [1] investigated the optimal implementation of distributed storage resources in IEEE® 123 node distribution test system with intelligent load shedding scheme to minimize the societal costs of blackouts. Papers [2–3] proposed and developed a new software planning tool from the aspect of overall network costs for distribution networks to define the placement, rating, and control strategies of distributed storage systems. In paper [4], the quantitative voltage stability index is proposed and improved in the IEEE 14 bus system by adding superconducting magnetic energy storage (SMES) systems. Genetic algorithm is adopted to solve the optimal locations for SMES. Paper [5] focuses on the use of energy storage with smart PV inverters in a distribution system, and assesses the impact of the placement and voltage regulation on the profitability of energy storage. A genetic algorithm-based approach is proposed in paper [6] to optimize the placement of a hybrid PV-Wind-Storage system in order to maximize the annual net profit.

This paper is a follow-up work to [9] that studied the generation capacity sizing to ensure power quality. In this paper, a technique is introduced to find the best location for an energy storage system in a microgrid to support the voltage and frequency profile. A voltage sensitivity study is conducted and four sensitivity indexes derived from Jacobean matrix are proposed and adopted to determine the candidate locations for energy storage devices. Various scenarios and cases are discussed, simulated, and compared for all the selected candidates in the proposed microgrid. Finally, the utility power quality indexes are calculated for various cases using the model developed in papers [7–9] to evaluate and compare for our system. The details and constraints of the components, including generations, loads, energy storage, and controls, have been considered in the models.



Powering Business Worldwide

Problem statement

A microgrid system based on IEEE 34 bus with high renewable energy penetration is proposed and studied in [7–9]. **Figure 1** shows the configuration of the microgrid. The original system is 60 Hz, 24.9 kV, 12 MVA with different fixed loads connected to the utility main at bus 800 and no distributed generations (DG) on the system [10]. In order to match the properties of the system with a microgrid under construction at Fort Sill, OK, the nominal voltage of the system is changed to 12 kV and other components of the system, including loads and line impedances, have been scaled accordingly. Four types of power sources are added: a 250 kW solar PV plant, two 750 kW wind turbines, a 1.5 MVA natural gas generator, and two 250 kW, 500 kWh zinc-bromide energy storage elements. The modeling and capacity design for these sources have been presented in [7–9].

A system collapse case has been observed and discussed in previous papers, which signifies the issue of placement and sizing of energy storage systems. Wrong placement of energy storage not only increases the overall microgrid costs but also the risks of low voltage and/or high voltage issues that may damage other devices in the microgrid. Most microgrids are built at low and medium voltage levels, where the distribution lines have significant impedances. Charging and discharging the energy storage in some instances may create voltage instability. In addition, the capability of the energy storage to support the voltage and frequency in the microgrid can be undermined. The strategic storage location and size also determine the threshold for renewable energy penetration, and the so-called stable operation (voltages and frequency) of a system [12]. Having an oversized storage connected at a randomly selected bus within a considerably large sized microgrid will not intrinsically have the best impact in terms of stability on the rest of the buses. The energy storage system must help supply the critical loads in the case of a shortage from the utility grid, but it has to be located properly to regulate both active/reactive power without an adverse impact on the voltage or frequency. The proper placement also enables the system to alleviate the voltage problems at various buses with smaller current flow from the storage element.

Proposed technique

The voltage sensitivity study is widely used in power system analysis to identify the relationships between voltage magnitude and active/reactive power at a particular bus. These relationships are usually depicted in so-called P-V and Q-V curves. In a transmission system, a Q-V curve is commonly adopted and studied to evaluate the impact of the reactive power on voltage magnitude in terms of dQ/dV [13], as it possesses a good linearity in an acceptable range deriving from the natural property of the overhead transmission line that the inductance is far greater than resistance. By contrast, active power has a negligible impact on the voltage magnitude, which is the reason that various types of reactive power suppliers, so-called reactive power compensators (such as SVC, STATCOM, synchronous condenser, and so on), are installed in the transmission system to supply and stable the system voltage.

However, in the distribution system, the relationship between voltage magnitude and active/reactive power is not as straightforward as that in the transmission system, because the cable selected for low and medium voltage systems has a significant resistance component. Therefore, it is necessary to have not only a reactive power supplier but also an active power supplier (distributed energy storage devices) installed in the system properly. A voltage sensitivity analysis for a distribution system, particularly for a microgrid, becomes challenging because of the coupled impact of active and reactive power on bus voltages.

In this paper, four indexes derived from Newton-Raphson power flow calculation are proposed and used for evaluating the sensitivity of PQ nodes in the power network.

The active and reactive power equations for bus i are computed as [11]:

$$P_i = V_i^2 G_{ii} + \sum_{\substack{j=1 \\ j \neq i}}^N |V_i V_j Y_{ij}| \cos(\theta_{ij} - \delta_i + \delta_j) \quad (1)$$

$$Q_i = -V_i^2 B_{ii} - \sum_{\substack{j=1 \\ j \neq i}}^N |V_i V_j Y_{ij}| \sin(\theta_{ij} - \delta_i + \delta_j) \quad (2)$$

In this equation, P_i and Q_i are injection active and reactive power of bus i , respectively. V_i and V_j are the voltage amplitude of bus i and j , respectively. Y_{ij} represents mutual-admittance. G_{ii} and B_{ii} are conductance and susceptance components of self-admittance at bus i . θ_{ij} represents the polar angle of self-admittance at branch i to j . δ_i and δ_j are the voltage angles at bus i and bus j , respectively.

By differentiating equations (1) and (2) with respect to voltage angles and magnitudes, the famous Newton-Raphson power flow equation is obtained in equation (3), where $[J]$ is Jacobian matrix containing partial derivatives of active power and reactive power with respect to voltage angles and magnitudes:

$$\begin{bmatrix} \Delta P \\ \Delta Q \end{bmatrix} = \begin{bmatrix} J_1 & J_2 \\ J_3 & J_4 \end{bmatrix} \begin{bmatrix} \Delta \delta \\ \Delta V \end{bmatrix} \quad (3)$$

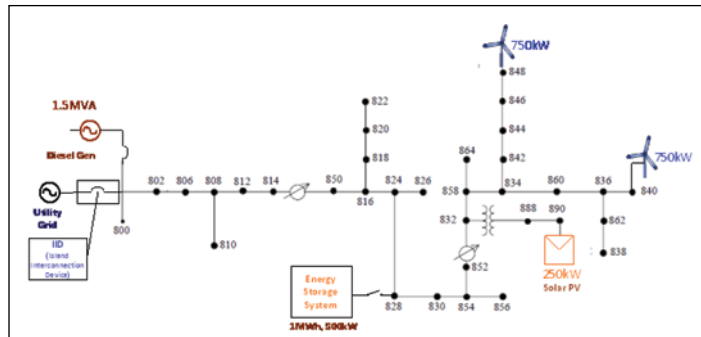


Figure 1. The Configuration of the Microgrid Studied in This Paper

Equation (3) is used to solve the power flow in a power system, while also looking to solve voltage sensitivity analysis increments of voltage angles and magnitudes. Therefore, a reversed calculation is proposed in this paper. The equation is shown in (4), where $[U]$ is defined as inverse Jacobian matrix. It also has four components, shown in equations (5–8):

$$\begin{bmatrix} \Delta\delta \\ \Delta V \end{bmatrix} = \begin{bmatrix} U_1 & U_2 \\ U_3 & U_4 \end{bmatrix} \begin{bmatrix} \Delta P \\ \Delta Q \end{bmatrix} \quad (4)$$

$$U_1 = \begin{bmatrix} \frac{\partial\delta_2}{\partial P_2} & \frac{\partial\delta_2}{\partial P_3} & \dots & \frac{\partial\delta_2}{\partial P_n} \\ \vdots & \vdots & \ddots & \vdots \\ \frac{\partial\delta_n}{\partial P_2} & \frac{\partial\delta_n}{\partial P_3} & \dots & \frac{\partial\delta_n}{\partial P_n} \end{bmatrix} \quad (5)$$

$$U_2 = \begin{bmatrix} \frac{\partial\delta_2}{\partial Q_2} & \frac{\partial\delta_2}{\partial Q_3} & \dots & \frac{\partial\delta_2}{\partial Q_n} \\ \vdots & \vdots & \ddots & \vdots \\ \frac{\partial\delta_n}{\partial Q_2} & \frac{\partial\delta_n}{\partial Q_3} & \dots & \frac{\partial\delta_n}{\partial Q_n} \end{bmatrix} \quad (6)$$

$$U_3 = \begin{bmatrix} \frac{\partial|V_2|}{\partial P_2} & \frac{\partial|V_2|}{\partial P_3} & \dots & \frac{\partial|V_2|}{\partial P_n} \\ \vdots & \vdots & \ddots & \vdots \\ \frac{\partial|V_n|}{\partial P_2} & \frac{\partial|V_n|}{\partial P_3} & \dots & \frac{\partial|V_n|}{\partial P_n} \end{bmatrix} \quad (7)$$

$$U_4 = \begin{bmatrix} \frac{\partial|V_2|}{\partial Q_2} & \frac{\partial|V_2|}{\partial Q_3} & \dots & \frac{\partial|V_2|}{\partial Q_n} \\ \vdots & \vdots & \ddots & \vdots \\ \frac{\partial|V_n|}{\partial Q_2} & \frac{\partial|V_n|}{\partial Q_3} & \dots & \frac{\partial|V_n|}{\partial Q_n} \end{bmatrix} \quad (8)$$

U_1 , U_2 , U_3 , and U_4 naturally represent the voltage change (both angle and magnitude) per increment of power (both active and reactive) not only on the same bus, but also represent the impacts on other buses. They contain all the information about system line structure and configuration. However, they are hardly analyzed and criticized when the system is large and complex. Therefore, to meet the objective of voltage assessment while simplifying the analysis, four voltage sensitivity indexes are defined in equations (9–12). These indexes are the summation of the columns of the inverted Jacobean matrix divided by the number of nodes. They define a mathematical weighted measurement to indicate whether a particular node has a significant contribution to the system voltages on average when an energy storage device is installed at that location.

$$\text{Index}_{1_i} = \frac{\sum_{k=1}^n \frac{\partial\delta_i}{\partial P_k}}{n} \quad (9)$$

$$\text{Index}_{2_i} = \frac{\sum_{k=1}^n \frac{\partial|V_i|}{\partial P_k}}{n} \quad (10)$$

$$\text{Index}_{3_i} = \frac{\sum_{k=1}^n \frac{\partial\delta_i}{\partial Q_k}}{n} \quad (11)$$

$$\text{Index}_{4_i} = \frac{\sum_{k=1}^n \frac{\partial|V_i|}{\partial Q_k}}{n} \quad (12)$$

Candidate bus selection

The flow chart of the proposed methodology is depicted in **Figure 2**. The steady state planning methodology calculates the indexes once the Newton-Raphson method converges to meet the requirements of the power flow. A change in the loading condition is applied at a selected node in the system and the indexes are recalculated. After following this procedure for various loading conditions, the voltage sensitivity indexes for each node are obtained.

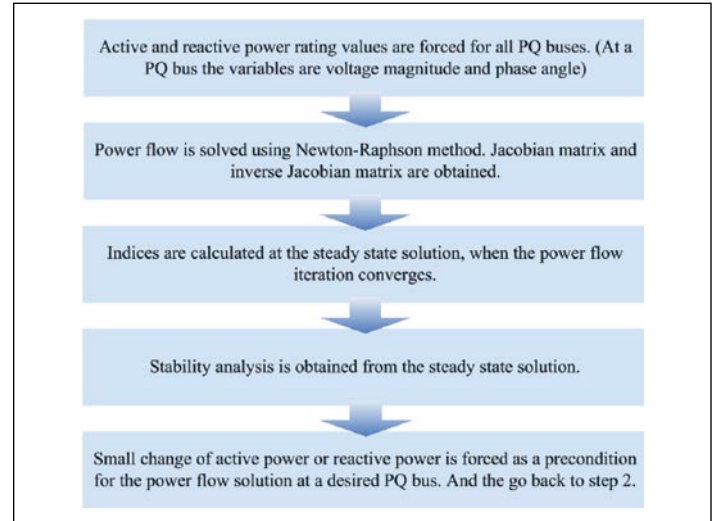


Figure 2. Diagram of the Process Used to Calculate the Indexes

Figure 3 shows curves of four indexes with respect to different loading conditions for the four selected buses after applying the proposed method to the microgrid. At first glance, the four curves look identical, but when zoomed-in they are different. The explanation and analyses of the curves, as well as the selected zoomed in pictures, will be discussed further. Before that, it is important to mention that the microgrid studied in the paper is a three-phase unbalanced system. There are several single- and two-phase branches. Because the energy storage systems should be installed at three-phase buses, and because the Newton-Raphson method is suitable for balanced systems, all the single- and two-phase branches are pruned, and an equivalent three-phase balancing modification is applied. The comparison of bus voltages (three-phase) per unit between original and balanced systems is shown in **Table 1**. The error is negligible, so the approximation is acceptable.

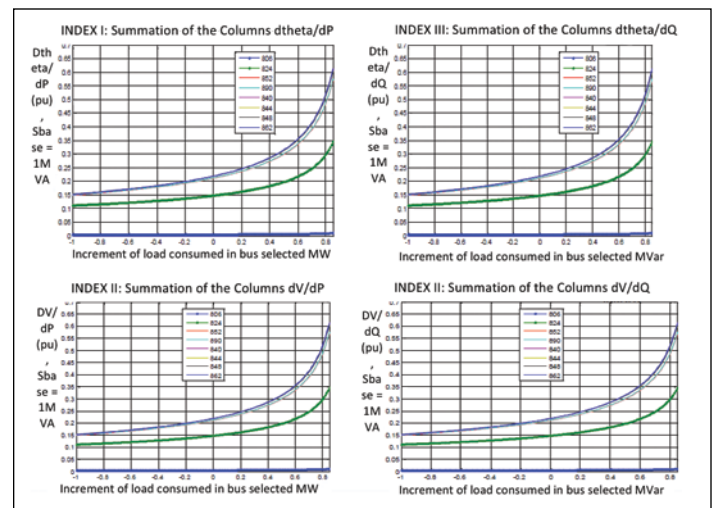


Figure 3. Curves of Four Indexes for the Microgrid with Respect to Different Loading Conditions

Results from modeling the case in PSCAD

In order to examine and evaluate the selected candidates obtained from the proposed methodology, various simulations and tests are conducted. The system is modeled in PSCAD. The detailed system configuration and transmission line information are described in [7–9]. The model offers a wide variety of detailed models, such as voltage regulators, unbalanced transmission lines, different types of loads, and various generations and their controls, including wind power, solar PV, energy storage devices, and diesel generators. The main advantage of using PSCAD is that a real-time simulation result can be obtained to assess the effects of storage in different locations with consideration to the controls and operations of the system.

The microgrid operation was tested and analyzed in four different operation modes, defined as [15] island mode, grid-connected mode, transition from grid-connected to island mode, and transition from island mode to grid-connected mode. Each one of these modes has its own power quality issues that affect the stability of the system, and primarily the voltage stability.

Discharging at 300 kW for a low voltage scenario in island mode

First, a 300 kW discharging for energy storage system at four locations in island mode is studied. The one-line diagram of the microgrid and four candidate locations are shown in **Figure 6**.

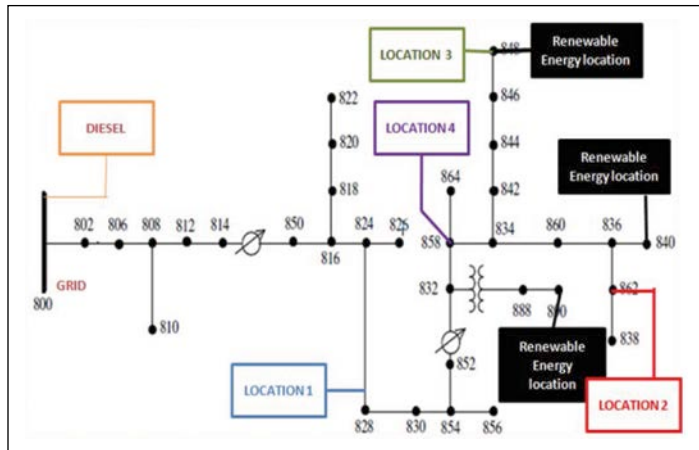


Figure 6. One-Line Diagram of the Microgrid with Four Selected Locations

A 1.4 MW nominal load is considered during simulation. No renewable generations are providing power to the system, as this test focuses on a low voltage scenario. A 500 kW ZBB battery equipped with an inverter interfaces to the microgrid at four different locations. The voltage values are monitored across all three-phase buses of the system, before and after the battery is discharged. These voltage results are captured once the steady state has been achieved.

Figure 7 shows the three-phase average voltage change per unit, when the battery is discharging at 300 kW (60% of the rated power). From the three-dimensional figure, it can be observed that location I has the lowest increase in voltage throughout all buses. locations II, III, and IV have a bigger increase in voltage as the battery is discharged.

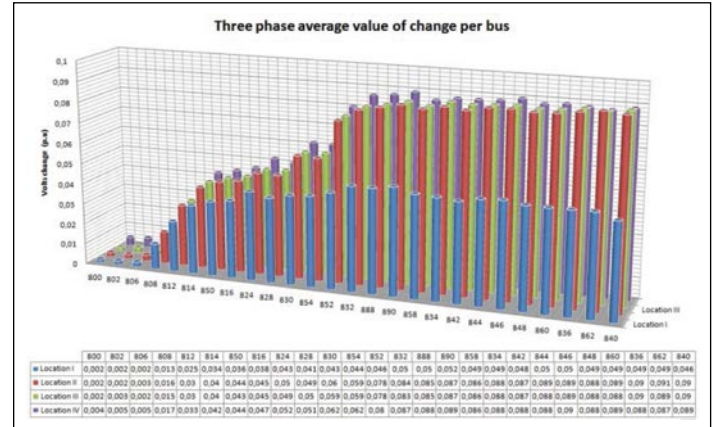


Figure 7. 3D Chart of Nodal Voltage Changes When Battery is Discharging at 300 kW in Island Mode at Selected Locations

Locations II, III, and IV have similar performances. An average of all bus voltage change is computed to determine which location is better and more effective. The results are shown and compared in **Figure 8**, where locations II and IV are the best choices.

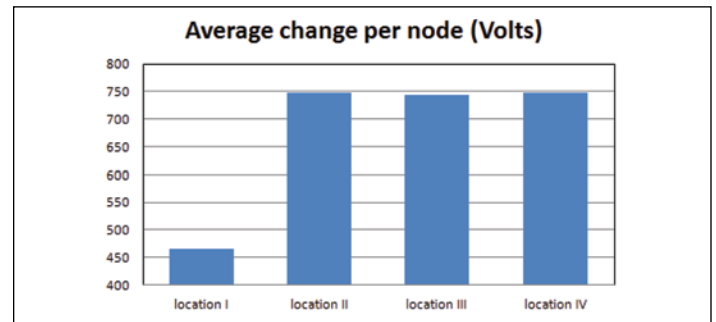


Figure 8. Average Changes per Node When Battery is Discharging at 300 kW in Island Mode at Selected Four Locations

In addition, the power quality indexes, namely SAIDI, SAIFI, and CAIDI, are calculated. These parameters are widely used by utility companies to evaluate power quality and reliability. SAIDI is the average outage duration for each customer served. SAIDI is measured in units of time, often minutes. It is usually measured over the course of a year, and the median value for North American utilities is around 1.50 hours. It is described as follows:

$$SAIDI = \frac{\text{Total duration of customer interruptions}}{\text{Total number of customers served}}$$

SAIFI is the average number of interruptions that a customer would experience. SAIFI is measured in units of interruptions per customer. It is usually measured over the course of a year, and the median value for North American utilities is approximately 1.10 interruptions per customer. SAIFI is described as:

$$SAIFI = \frac{\text{Total number of customer interruptions}}{\text{Total number of customers served}}$$

CAIDI is the Customer Average Interruption Duration Index and is described as:

$$CAIDI = \frac{\text{Total duration of customer interruptions}}{\text{Total number of customer interruptions}} = \frac{SAIDI}{SAIFI}$$

The results obtained for the 24-hour simulation are given in **Table 4**. Coherently to **Table 3**, location II is the best solution that exhibits fewer customer interruptions than other locations.

Table 4. Comparison of Power Quality Indexes

	Location I	Location II	Location III	Location IV	Units
SAIDI	17.1247	5.8517	Unstable	5.9258	min
SAIFI	20.41	1.7647	Unstable	1.94117	—
CAIDI	0.838963	0.301568	Unstable	0.32756	min

Conclusions

This paper presented voltage sensitivity indexes derived from the inverse of Jacobian matrix from Newton-Raphson power flow analysis. The indexes imply the sensitivity of nodal voltages (both angles and magnitudes) in terms of four components: $\Delta V/\Delta P$, $\Delta V/\Delta Q$, $\Delta \delta/\Delta P$, and $\Delta \delta/\Delta Q$. By calculating these indexes, the candidate buses for installing the energy storage devices are found. To test and demonstrate the methodology, three cases have been studied. The results from the sensitivity analysis and case studies indicate the same conclusion, that locations II, III, and IV are better than the original selection in previous studies [7–9]. After applying a 24-hour time-sequence simulation, location II is found to be the best solution.

Acknowledgment

This material is based upon work supported by the U.S. Army Corps of Engineers (ERDC/CERL) under Contract No. W9132T-11-C-0022. Any opinions, findings, conclusions, or recommendations expressed in this material are those of the author(s) and do not necessarily reflect the views of the U.S. Army Corps of Engineers.

References

1. J. M. Gantz, M. M. Amin, "Optimal mix and placement of energy storage systems in power distribution networks for reduced outage costs," in Proc. IEEE ECCE 2012, Raleigh, NC
2. G. Celli, S. Mocci, F. Pilo, M. Loddo, "Optimal integration of energy storage in distribution networks," in Proc. IEEE PowerTech 2009, Bucharest, Romania
3. G. Carpinelli, G. Celli, S. Mocci, F. Mottola, F. Pilo, D. Proto, "Optimal Integration of Distributed Energy Storage Devices in Smart Grids," IEEE Transactions on Smart Grid, vol. PP, issue 99, pp: 1-11, 2013.
4. X. Huang, G. Zhang, L. Xiao, "Optimal Location of SMES for Improving Power System Voltage Stability," IEEE Transactions on Applied Superconductivity, vol. 20, pp 1316-1319, 2010.
5. A. K. Barnes, J. C. Balda, A. Escobar-Mejia, S. O. Geurin, "Placement of energy storage coordinated with smart PV inverters," in Proc. IEEE ISGT 2012, Washington D.C.
6. J. Zou, K. Zhou, K. Lei, Z. Zhang, X. Xin, "A Method to Optimize the Placement of PV-Wind-Storage Hybrid System," in Proc. IEEE APPEEC 2012, Shanghai, China.
7. Q. Fu, L. F. Montoya, A. Solanki, A. Nasiri, V. Bhavaraju, T. Abdallah, D. C. Yu, "Generation Capacity Design for A Microgrid for Measurable Power Quality Indexes," in Proc. IEEE ISGT 2012 Conf., Washington, D.C.
8. A. Solanki, Q. Fu, L. F. Montoya, A. Nasiri, V. Bhavaraju, T. Abdallah, D. C. Yu, "Managing Intermittent Renewables in A Microgrid," in Proc. IEEE ISGT 2012 Conf., Washington, D.C..
9. Q. Fu, L. F. Montoya, A. Solanki, A. Nasiri, V. Bhavaraju, T. Abdallah, D. C. Yu, "Microgrid Generation Capacity Design With Renewable and Energy Storage Addressing Power Quality and Surety," IEEE Transactions on Smart Grid, vol. 3, pp. 2019-2027, 2012.
10. R.C. Dugan, W. H. Kersting, "Induction machine test case for the 34-bus test feeder – description," IEEE Power Engineering Society General Meeting, 2006, Montreal, Quebec.
11. J. J. Grainger, W. Stevenson, "Power System Analysis," McGraw-Hill Science.
12. C. Hill, D. Chen, "Development of a real-time testing environment for battery energy storage systems in renewable energy applications," in Proc. IEEE PESGM 2011, Detroit, MI.
13. Q. Fu, D. Yu, J. Ghorai, "Probabilistic load flow analysis for power systems with multi-correlated wind sources," in Proc. IEEE PESGM 2011, Detroit, MI.
14. A. Keane, M. O'Malley, "Optimal Allocation of Embedded Generation on Distribution Networks," IEEE Transactions on Power Systems, vol. 20, pp. 1640-1646.
15. V. Bhavaraju, A. Nasiri, Q. Fu, "Multi-Inverter Controls and Management of Energy Storage for Microgrid Islanding," The Electricity Journal, vol. 25, pp. 36-44.

Eaton
1000 Eaton Boulevard
Cleveland, OH 44122
United States
Eaton.com

© 2014 Eaton
All Rights Reserved
Printed in USA
Publication No. WP083008EN / Z14978
May 2014